

PDF hosted at the Radboud Repository of the Radboud University Nijmegen

The following full text is a publisher's version.

For additional information about this publication click this link.

<http://hdl.handle.net/2066/60340>

Please be advised that this information was generated on 2019-02-21 and may be subject to change.

Transitions Driven by a Missing Frequency

Andreas Gürtler¹ and Wim J. van der Zande^{1,2}

¹*FOM Institute for Atomic and Molecular Physics, Kruislaan 407, 1098 SJ Amsterdam, The Netherlands*

²*Department of Molecular and Laser Physics, Institute for Molecules and Materials, Radboud University, Nijmegen, The Netherlands*

(Received 18 March 2004; published 5 October 2004)

We demonstrate an intricate combination of strong and weak interactions of a broadband half-cycle pulse with Rydberg atoms. A transition, which is resonant with a frequency that was taken out of the frequency spectrum, can be enhanced. In the experiment, the broadband ultrashort terahertz half-cycle pulse propagates through water vapor, which absorbs on discrete lines in the spectrum, thus removing frequencies from the spectrum. The resulting pulse interacts with a rubidium Rydberg atom, which has a resonant transition with one of the missing frequencies. Under certain conditions, the transition probability is enhanced although the associated frequency was missing in the spectrum.

DOI: 10.1103/PhysRevLett.93.153002

PACS numbers: 32.80.Rm, 32.80.Qk

In many situations where light and matter interact, the interaction is governed by the spectrum of the light and the frequencies of possible transitions of the matter in question. If the intensity of the light becomes very high, multiphoton transitions can become important, ultimately reaching the situation that the electric field of the light suppresses the binding Coulomb forces as happens, e.g., in above-threshold ionization [1,2] or in the interaction of Rydberg atoms with strong half-cycle electric field pulses [3–6]. In another class of light-matter interactions, for example, in stimulated Raman adiabatic passage, the coherent properties of light are employed [7]. In this Letter, we discuss an interesting case which combines all three of these aspects, the interaction of Rydberg atoms with terahertz half-cycle pulses (HCP), which have a spectrum with “gaps” as a result of absorption in water vapor. If a transition in the Rydberg atom is resonant with a gap in the THz pulse spectrum, intuition tells us that this transition is less likely to happen than in the case where the resonant frequency is still in the spectrum. On second thought, the interaction of strong ultrashort half-cycle pulses with Rydberg atoms, which are highly susceptible to electric fields, is almost always strongly driven and poorly described by a single-photon picture. In fact, this interaction is frequently described as a semiclassical “momentum kick” $\Delta\vec{p} = e \int \vec{E}_{\text{HCP}}(t) dt$ to a free electron with charge e due to the electric field $\vec{E}_{\text{HCP}}(t)$ of the half-cycle pulse [3]. The energy lost or gained in the impulsive approximation is then $\Delta E = \frac{1}{2m} (2\vec{p} \cdot \Delta\vec{p} + \Delta\vec{p}^2)$, where \vec{p} is the initial momentum and m is the mass of the electron. However, the momentum kick picture does not take into account possible single-photon transitions. In this Letter, we demonstrate that half-cycle pulses, which propagated through laboratory air containing water vapor and are reshaped by absorption and dispersion, efficiently drive single-photon transitions at a missing frequency. We show where this contribution is visible above the strong multiphoton back-

ground. We illustrate the single-photon nature of this interaction by measuring the transition frequency and width of a rotational water line in the far infrared.

Figure 1(a) shows the electric field of a pure Gaussian half-cycle pulse with the Fourier transform given in Fig. 1(b). The zero-frequency component of pure half-cycle pulses cannot propagate. Therefore, HCPs develop a long “tail” of opposite polarity during propagation such that in the far field, the integral of the electric field is zero. The effects of this impurity on Rydberg atom excitation have been investigated earlier [4,6,8] and are not the subject of this Letter. THz half-cycle pulses are being used for rotational spectroscopy of molecules in the gas phase [9,10]. The absorption of frequencies and the following free-induction decay of the excited molecules reshape the THz pulse [9]. For low intensities, the reshap-

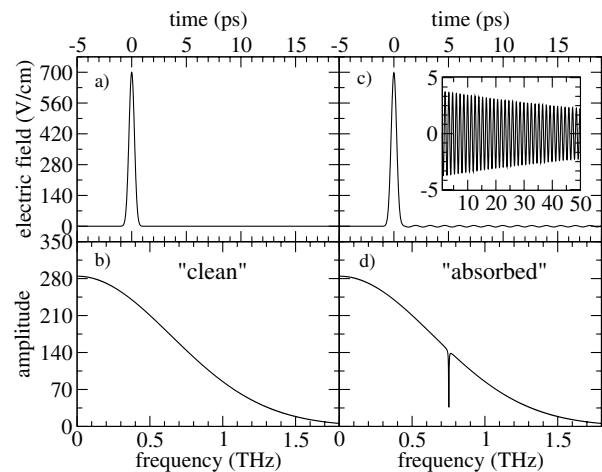


FIG. 1. Electric field (a) and Fourier transform (b) of a clean half-cycle pulse with a duration of 0.65 ps. (c) Electric field after propagation through a medium with an absorbing line at 752 GHz calculated by linear dispersion theory. The inset shows a zoom of the low-amplitude oscillatory tail. (d) Frequency spectrum of the absorbed pulse (c).

ing of the electric field after propagation through a medium which absorbs on discrete lines is well described by linear dispersion theory and can be written as [10]

$$\varepsilon_{\text{THz}}(z, t) = \int \tilde{\varepsilon}_{\text{THz}}(\omega) e^{-i(\omega t - k_0 z)} e^{i\Delta k(\omega)z} e^{-\alpha(\omega)z/2} d\omega,$$

where $k = n\omega/c$. $\Delta k(\omega)$ and $\alpha(\omega)$ are the frequency-dependent dispersion and power absorption coefficient, respectively. $\tilde{\varepsilon}_{\text{THz}}(\omega)$ is the Fourier transform of the electric field of the half-cycle pulse at $z = 0$. In the simple single-line absorber model depicted in Fig. 1, Δk and α are assumed to have Lorentzian dispersion and absorption line shapes. Figure 1(d) shows the predicted frequency spectrum of the half-cycle pulse after propagation through a 40 cm sample of a medium which absorbs on the frequency of the H_2O (J, K_a, K_c) = (2 1 1) \leftarrow (2 0 2) rotational transition at 752 GHz (25.08 cm^{-1}) [11]. The time-domain pulse shape obtained by an inverse Fourier transform is shown in Fig. 1(c). The shape of the short half cycle is not appreciably changed. Following the short half cycle, there is a low-amplitude oscillatory tail stemming from the free-induction decay of the excited absorber which can extend up to several hundred picoseconds after the 0.65 ps half-cycle pulse. The decay time for the transient is ~ 75 ps for the 752 GHz line used in Fig. 1. In the following, we refer to pulses like the one shown in Fig. 1(a) as “clean” pulses as opposed to “absorbed” pulses as shown in Fig. 1(c).

The experiment is performed in a vacuum chamber (10^{-7} mbar). We excite rubidium atoms from a resistively heated oven into the $25D$ Rydberg state in a two-photon transition using a nanosecond dye laser. The excitation takes place between two capacitor plates which can be biased by a voltage to produce an electric field in the interaction region. The upper plate contains a hole covered by a grid. After interaction with the THz half-cycle pulses, which are produced in a biased large-aperture GaAs antenna illuminated by 800 nm, 100 fs pulses from a regeneratively amplified Ti:sapphire laser system [12], the Rydberg population is probed by state-selective field ionization (SFI). To that end, a slow voltage ramp is applied to the lower capacitor plate. The field at which a state ionizes is a measure for the state’s principal quantum number n [13]. The SFI field also pushes the ionized electrons towards a microchannel plate detector (MCP). The time of flight at which the electrons arrive gives the ionization field and, with it, the state distribution. The MCP signal is digitized by a fast digital oscilloscope and the traces are stored on a computer for further processing.

Before entering the vacuum chamber, the THz beam traverses a 40 cm tube which can be filled with air containing water vapor or flooded with dry nitrogen. To measure a line profile as shown in Fig. 2(a), the SFI traces are taken after exposing the Rydberg atoms to the THz beam which propagated through the tube containing water vapor. Then the static electric field is increased and the next trace is taken. As a background measure-

ment, the field scan is then repeated with the THz beam blocked. Then the water vapor tube is flooded with dry nitrogen and the measurement is repeated. The absorption data are then the difference in upper state population for the water vapor and nitrogen data, respectively.

Rydberg atoms, atoms in a highly excited electronic state, typically have multiple transitions in the bandwidth of a THz pulse. Transitions between Rydberg states can be tuned by means of Stark tuning [14]. The principle is depicted in Fig. 2(b). The figure shows the energy of rubidium Rydberg states around the $25D$ state as a function of an external electric field calculated using experimental quantum defects [15,16]. Fine structure was not included in the calculation and for the P states, the $P_{1/2}$ quantum defects were used. The $D_{3/2}$ and $D_{5/2}$ states are practically degenerate at these values of n . The energy of a Rydberg state in an external electric field depends on the value of the field. Figure 2(c) shows the energy difference between the $25D$ and the $28P$ state. Clearly, this energy difference can be tuned by changing the electric field. At a field of 61 V/cm [marked by an arrow in Fig. 2(b)], the

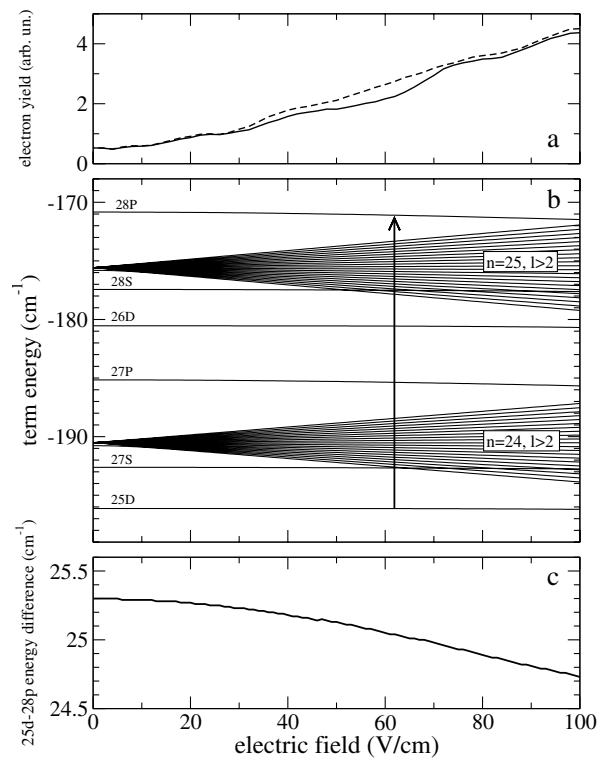


FIG. 2. (a) Measured $28P$ state population as a function of external electric field after exposure of an initially excited $25D$ state to THz pulses which propagated through air containing water vapor (dashed line) and dry nitrogen (solid line). (b) Calculated rubidium energy levels around the $25D$ state as a function of electric field. The arrow denotes the field where the $25D$ - $28P$ transition frequency equals 752 GHz. The quantum defects of P and D states are 2.65 and 1.35, respectively. (c) Energy difference between the Rb $25D$ and $28P$ states as a function of field.

transition energy is equal to that of an absorption line of gaseous water at 25.085 cm^{-1} ($\sim 752 \text{ GHz}$). Figure 2(a) shows the experimental population in the $28P$ state as a function of static electric field after an initially excited $25D$ state was exposed to a HCP that propagated through 40 cm of laboratory air containing water vapor (dashed line) and a HCP that propagated through 40 cm of dry nitrogen (solid line). Surprisingly, at 61 V/cm , when the $25D \rightarrow 28P$ transition is resonant with the water absorption line at 752 GHz , the absorbed pulse which actually has a hole in the spectrum at this frequency as shown in Fig. 1(d), transfers *more* population to the upper state than the clean pulse which has an intact spectrum.

In Fig. 3 we show results of a numerical integration of the time-dependent Schrödinger equation of a Rb $25D$ state in fields as shown in Fig. 1. The wave function is represented on a radial grid by a sum of angular wave functions, which are the product of a radial function and a spherical harmonic. The calculations were performed using a split-operator method. The Hamiltonian was split into two parts, the first representing the field-free atomic Hamiltonian in a Rb model potential, the second part representing the external fields [17].

In Fig. 3(a) the population in the $28P$ state during and after the HCP is plotted as a function of time for three HCP amplitudes. The peak of the HCP with a full width at half maximum of 0.65 ps is at 10 ps . The population oscillates in time with a frequency that depends on the HCP amplitude and the population after the pulse is over is a nontrivial function of the amplitude. In Fig. 3(b) the

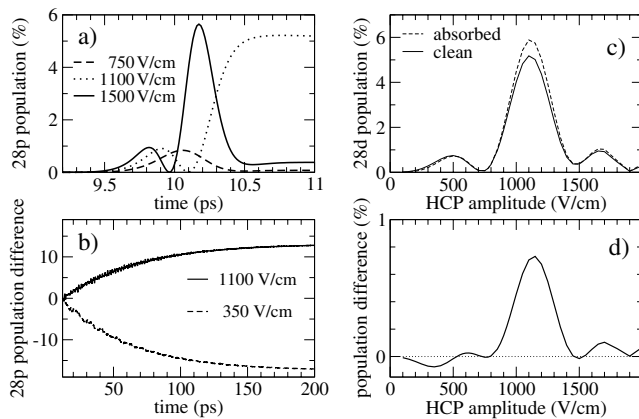


FIG. 3. (a) Calculated $28P$ state population in percent of the initial state population as a function of time *during* the half-cycle pulse which peaks at 10 ps (0.65 ps duration) for three HCP amplitudes. (b) Difference in $28P$ state populations excited by an absorbed and a clean HCP in percent of the clean upper state population for two HCP amplitudes as a function of time. (c) Asymptotic population in the $28P$ state in percent of the initial state population as a function of HCP amplitude after application of a HCP to an initial $25D$ state for a pure HCP (solid line) and a HCP after propagation through a medium which absorbs at the $25D \rightarrow 28P$ transition frequency (dashed line). (d) Difference of the curves in (c): $P_{\text{absorbed}} - P_{\text{clean}}$.

population difference of $28P$ population excited by clean pulses [Fig. 1(a)] and absorbed pulses [Fig. 1(c)] is shown as a function of time for HCP amplitudes of 350 and 1100 V/cm . In the field shown in Fig. 1(c), the weak oscillating tail contains the missing frequency, but with a phase shift of π , such that it interferes destructively with the same frequency component of the half-cycle pulse, leading to the spectrum shown in Fig. 1(d). In a linear interaction, we naturally expect that a frequency that is not contained in the spectrum does not drive a transition. The wave function excited by the half-cycle pulse is then out of phase with the coherent resonant tail of the pulse and the population is coherently driven back down rather than up, even though the initial ($25D$) state population exceeds the $28P$ state population by far. This behavior is shown by the dashed line in Fig. 3(b) for a 350 V/cm HCP amplitude. For very small HCP amplitudes ($\sim 10 \text{ V/cm}$) and excitation probabilities ($\sim 10^{-6}$), the excited fraction for the absorbed pulse after the pulse is ca. 25% of the clean pulse population as expected from the spectrum Fig. 1(d).

Even for moderate HCP amplitudes, the interaction of the HCP with the Rydberg state is highly nonlinear. The classical energy transfer ΔE then equals or exceeds the energies in the THz spectrum and the transition probability depends almost exclusively on the transition energy rather than the single-photon cross section of the transition. Note that all but the smallest HCP amplitudes are strong compared to typical fields in the Rydberg atom (a static field of $\geq 200 \text{ V/cm}$ already mixes the $25D$ state with the next higher-lying manifold of Stark states). In a nonlinear interaction, the created wave function does not necessarily have a destructive phase relationship with the oscillatory tail, such that this narrow-band feature can efficiently drive more population from the $25D$ to the $28P$ state. Naturally, this effect is limited by the fact that strong half-cycle pulses leave very little population in the initial $25D$ state [$\approx 6\%$ in the case of the 1100 V/cm trace in Fig. 3(b)]. Figure 3(c) shows the asymptotic population in the $28P$ state as a function of the HCP amplitude for clean and absorbed HCPs. The population shows clear oscillations with peak values that are much smaller than 1 and not constant. These oscillations are not adequately described by a generalized Rabi frequency. The ultrabroad bandwidth and the half-cycle shape of the radiation as well as the potentially large number of states involved complicate the situation. Population oscillations in HCP excitation have been predicted using semiclassical calculations [18] and have been observed experimentally [19]. Figure 3(d) shows the difference in the $28P$ state populations for both pulse shapes. The effect of the oscillatory tail clearly depends on the HCP amplitude. Only for low amplitudes ($\leq 500 \text{ V/cm}$) the upper state population is less for the spectrum which lacks the transition frequency. For a HCP amplitude of 1150 V/cm , the absorbed HCP transfers more population from the $25D$ to the $28P$ state than the clean HCP.

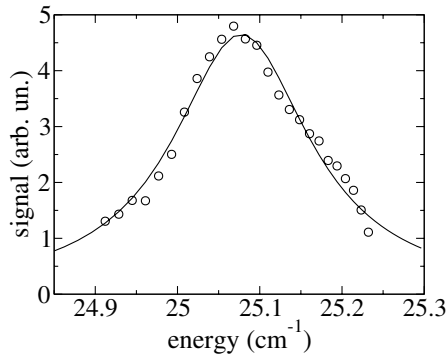


FIG. 4. Measured absorption line profile of the H_2O (J, K_a, K_c) = (2 1 1) \leftarrow (2 0 2) transition (circles) and Voigt profile fit to the data (line). The x axis is converted from field to energy using Fig. 2(c).

This situation can be compared with filtering by linear and nonlinear filters. Linear frequency filters, e.g., dichroic bandpass filters [20], will produce a gap in the spectrum when applied to a pulse like the one shown in Fig. 1(c). Nonlinear filters, e.g., ultrafast switchable mirrors switched on after the HCP or saturable absorbers, can produce a pulse with a *peak* at the absorbed frequency.

We use the sensitivity and the tunability of the Rydberg transitions to probe a single rotational transition in gaseous water. In Fig. 4, we show the measured line shape of the H_2O (J, K_a, K_c) = (2 1 1) \leftarrow (2 0 2) transition at 752 GHz. The line shape is obtained by plotting the difference in transition probability to the $28P$ state for a THz pulse which propagated through air containing water vapor and a reference pulse which propagated through dry nitrogen as a function of energy separation of the $25D$ and $28P$ states. Figure 4 shows the experimental water line data as a function of frequency (circles) along with a Voigt profile fit to the data (line). The values for the water line extracted from the fit are the line position at $\nu_0 = 25.078 \text{ cm}^{-1}$ with a half width half maximum of $\Delta\nu = 0.102 \text{ cm}^{-1}$. These values are in good agreement with line data from the HITRAN spectroscopic database: $\nu_0 = 25.085 \text{ cm}^{-1}$, $\Delta = 0.099 \text{ cm}^{-1}$ [11]. Uncertainties in the line position and width arise mainly from the error in the determination of the electric field and field inhomogeneities. The gradient of the curve plotted in Fig. 2(c) around 60 V/cm is about $0.008 \text{ cm}^{-1}/(\text{V}/\text{cm})$. We estimate our error in field to be on the order of 2%, yielding an error in line position of $\sim 0.01 \text{ cm}^{-1}$. Other sources of error are the accuracy of the level map calculation and fluctuations in the THz and dye laser intensity.

In conclusion, we have shown that the interaction of THz half-cycle pulses that contain narrow-band low-amplitude oscillations as a result of an absorption process results in an interesting interplay between strong and weak field effects in Rb Rydberg atoms. A transition can be driven more effectively when its transition frequency is missing in the THz spectrum. This can be

explained by the nonlinear interaction of the half-cycle pulse with the atom which creates a wave function that does not have a destructive phase relationship with the low-amplitude tail. This allows the oscillatory tail to excite more population rather than to deexcite, as it would in a linear interaction.

We thank F. Robicheaux for his code to integrate the Schrödinger equation, L. Kuipers for careful reading of the manuscript, and B.W. Shore and L. D. Noordam for helpful discussions. A. G. acknowledges support from the EU program HPRN-CT-1999-00129, COCOMO. This work is part of the research program of the “Stichting voor Fundamenteel Onderzoek der Materie (FOM),” which is financially supported by the “Nederlandse Organisatie voor Wetenschappelijk Onderzoek (NWO).”

-
- [1] P. Agostini, F. Fabre, G. Mainfray, G. Petite, and N. K. Rahman, *Phys. Rev. Lett.* **42**, 1127 (1979).
 - [2] T. F. Gallagher, *Phys. Rev. Lett.* **61**, 2304 (1988).
 - [3] R. R. Jones, D. You, and P. H. Bucksbaum, *Phys. Rev. Lett.* **70**, 1236 (1993).
 - [4] C. Wesdorp, F. Robicheaux, and L. D. Noordam, *Phys. Rev. Lett.* **87**, 083001 (2001).
 - [5] F. Robicheaux, *Phys. Rev. A* **56**, R3358 (1997).
 - [6] A. Wetzels, A. Gürtler, L. D. Noordam, F. Robicheaux, C. Dinu, H. G. Muller, M. J. J. Vrakking, and W. J. van der Zande, *Phys. Rev. Lett.* **89**, 273003 (2002).
 - [7] K. Bergmann, H. Theuer, and B. W. Shore, *Rev. Mod. Phys.* **70**, 1003 (1998).
 - [8] N. E. Tielking, T. J. Bensity, and R. R. Jones, *Phys. Rev. A* **51**, 3370 (1995).
 - [9] H. Harde, S. Keiding, and D. Grischkowsky, *Phys. Rev. Lett.* **66**, 1834 (1991).
 - [10] H. Harde, R. A. Cheville, and D. Grischkowsky, *J. Phys. Chem. A* **101**, 3646 (1997).
 - [11] L. S. Rothman *et al.*, *J. Quant. Spectrosc. Radiat. Transfer* **60**, 665 (1998), <http://cfa-www.harvard.edu/HITRAN>.
 - [12] D. You, R. R. Jones, P. H. Bucksbaum, and D. R. Dykaar, *Opt. Lett.* **18**, 290 (1993).
 - [13] T. F. Gallagher, *Rydberg Atoms* (Cambridge University Press, Cambridge, 1994).
 - [14] T. W. Ducas, W. P. Spencer, A. G. Vaidyanathan, W. H. Hamilton, and D. Kleppner, *Appl. Phys. Lett.* **35**, 382 (1979).
 - [15] M. L. Zimmerman, M. G. Littman, M. M. Kash, and D. Kleppner, *Phys. Rev. A* **20**, 2251 (1979).
 - [16] W. Li, I. Mourachko, M. W. Noel, and T. F. Gallagher, *Phys. Rev. A* **67**, 052502 (2003).
 - [17] F. Robicheaux, E. Oks, A. L. Parker, and T. Uzer, *J. Phys. B* **35**, 4613 (2002).
 - [18] C. D. Schwieters and J. B. Delos, *Phys. Rev. A* **51**, 1023 (1995).
 - [19] N. E. Tielking and R. R. Jones, *Phys. Rev. A* **52**, 1371 (1995).
 - [20] C. Winnewisser, F. Lewen, and H. Helm, *Appl. Phys. A* **66**, 593 (1998).